Site-Directed Fluorescence Labeling of a Membrane Protein with BADAN: Probing Protein Topology and Local Environment

Rob B. M. Koehorst, Ruud B. Spruijt, and Marcus A. Hemminga
Laboratory of Biophysics, Wageningen University, Wageningen, The Netherlands

ABSTRACT The work presented here describes a new and simple method based on site-directed fluorescence labeling using the BADAN label that permits the examination of protein-lipid interactions in great detail. We applied this technique to a membrane-embedded, mainly α-helical reference protein, the M13 major coat protein. Using a high-throughput approach, 40 site-specific cysteine mutants were prepared of the 50-residues long protein. The steady-state fluorescence spectra were analyzed using a three-component spectral model that enabled the separation of Stokes shift contributions from water and internal label dynamics, and protein topology. We found that most of the fluorescence originated from BADAN labels that were hydrogen-bonded to water molecules even within the hydrophobic core of the membrane. Our spectral decomposition method revealed the embedment and topology of the labeled protein in the membrane bilayer under various conditions of headgroup charge and lipid chain length, as well as key characteristics of the membrane such as hydration level and local polarity, provided by the local dielectric constant.

INTRODUCTION

In our previous work on the development of site-directed fluorescent methods to determine the structure of membrane proteins, we used AEDANS as a label. For these studies, the M13 major coat protein was selected as a reference protein, because its membrane-bound properties have been described in several biophysical studies (for a review, see Stopar et al. (1)). Moreover, under the experimental conditions used for the fluorescence experiments, our findings were not complicated by protein-protein interactions (2) and environmental stress (3). In these studies, we demonstrated that the coat protein is a single membrane spanning almost straight α-helical protein (3–5) that did not differ much from the structure in the intact phage (6). AEDANS has several physicochemical properties that make it a useful label for such investigations: 1), the fluorescent spectrum is a simple line shape of which the position is sensitive to the environmental polarity (i.e., it is an environmental probe) (7–10); 2), the AEDANS linker is sufficiently long and flexible to enable the probe to sense the global environment and not local molecular effects; and 3), the linker flexibility enables accurate Förster (or fluorescence) resonance energy transfer experiments to be carried out on the donor-acceptor pair Trp-AEDANS using an averaged orientation factor $\kappa^2 = 2/3$ (3–5,11). From the environmental properties of the AEDANS label, the membrane embedment also was found, resulting in a slightly tilted protein topology (10).

The BADAN label (Fig. 1) is a good alternative for AEDANS; because it has a shorter linker, its fluorescence spectra can reflect more local molecular details. In this respect, BADAN resembles Aladan, a synthetic amino acid that, on incorporating into a protein, has a BADAN-like chromophore at a short distance to the protein backbone (12,13). Therefore, it could be a more accurate monitor for the direct environment of the labeled site. From a photophysical point of view, BADAN is similar to the well-known polarity probes PRODAN and LAURDAN that have been used in several membrane studies. Both probes demonstrate a so-called ''dual fluorescence'' behavior that is explained by the presence of at least two excited states of which one is denoted as a locally excited or Franck Condon state and the other is denoted as an ICT state (14–19). In general, the solvent-dependent red shift of the fluorescence of these labels is, at least partly, ascribed to relaxation of the polar ICT state by reorientation of solvent dipoles. However, in several studies, both of experimental and theoretical nature, the involvement of planar as well as twisted ICT states (planar intramolecular charge transfer state and twisted intramolecular charge transfer state, respectively) were discussed (13,17,20,21). Twisting in the excited state (i.e., rotation or wobbling of the propanoyl moiety with respect to the aromatic ring (*arrow* in Fig. 1)) is

Submitted November 15, 2007, and accepted for publication December 21, 2007.

Address reprint requests to Marcus A. Hemminga, Laboratory of Biophysics, Wageningen University, PO Box 8128, 6700 ET Wageningen, The Netherlands. Office: Dreijenlaan 3, 6703 HA Wageningen, The Netherlands. Tel.: 31-317-482044; Fax: 31-317-482725; E-mail: marcus.hemminga@wur.nl; web site: http://ntmf.mf.wau.nl/hemminga/.

Abbreviations used: BADAN, 6-bromo-acetyl-2-dimethylamino-naphtalene; 16:1PC, 1,2-dipalmitoleoyl-*sn*-glycero-3-phosphocholine; 18:1PC, 1,2-dioleoyl-*sn*-glycero-3-phosphocholine; 18:1PG, 1,2-dioleoyl-*sn*-glycero-3-[phospho-rac-(1-glycerol)]; 20:1PC, 1,2-dieicosenoyl-*sn*-glycero-3-phosphocholine; 14:1PC, 1,2-dimyristoleoyl-*sn*-glycero-3-phosphocholine; Aladan, artificial fluorescent amino acid; AEDANS, *N*-(acetylaminoethyl)-5-naphthylamine-1-sulfonic acid; $HICT_i$, hydrogen-bonded intramolecular charge transfer state in an immobilized environment; $HICT_m$, hydrogen-bonded intramolecular charge transfer state in a mobile environment or with local mobility; ICT, intramolecular charge transfer state; LAURDAN, 6-lauroyl-2-(dimethylamino)-naphthalene; PICT, planar intramolecular charge transfer state; PRODAN, 6-propionyl-2-(dimethylamino)naphthalene; TICT, twisted intramolecular charge transfer state.

Editor: Peter Tieleman.

0006-3495/08/05/3945/11 $2.00

doi: 10.1529/biophysj.107.125807

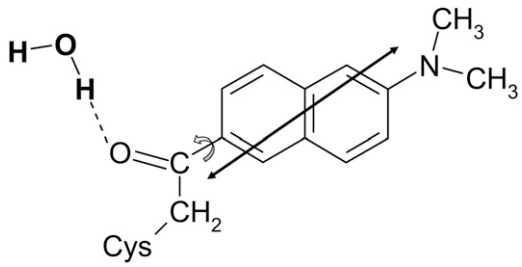

FIGURE 1 Structural formula of the fluorescence label BADAN covalently linked to the cysteine sulfur and hydrogen-bonded to a water molecule via its carbonyl oxygen (*dashed line*). The arrow around the bond between the dimethylamino group and the aromatic ring indicates label dynamics (rotation or wobbling) in the excited state. The large arrow represents the excitation dipole (16,29), with its orientation being parallel to the above-mentioned rotation axis.

thought to be the most probable mechanism for internal label dynamics (17,21).

From studies of PRODAN and LAURDAN in lipid bilayer systems, it is generally accepted that the solvent contribution to the observed shift of the fluorescence spectrum concerns the relaxation of their relatively polar-excited state by surrounding water dipoles (16,19,22–27). Thus, by using the BADAN label in site-directed studies of membrane-proteins, it could be expected that it would provide more physicochemical details about the protein-lipid-water system compared to the AEDANS label.

In this article, we present steady-state fluorescence data of site-directed BADAN-labeled M13 coat protein mutants reconstituted in lipid bilayers under various conditions of headgroup charge and lipid chain length. Analysis of the fluorescent data revealed the embedment and topology of the labeled protein in the membrane bilayer under various conditions of headgroup charge and lipid chain length, as well as key characteristics of the membrane, such as hydration level and local polarity.

EXPERIMENTAL

Sample preparation

In a high-throughput approach, a total of 40 site-specific cysteine mutants of M13 major coat protein were prepared, purified, and labeled with BADAN (Invitrogen, Molecular Probes, Carlsbad, CA), a process similar to that described by a previous study in which labeling was performed with *N*-(iodoacetylaminoethyl)-5-naphthylamine-1-sulfonic acid) (8). These mutants covered 80% of the total number of amino acid residues in the primary sequence of the 50-residues long protein. BADAN-labeled M13 coat protein mutants were reconstituted into phospholipid bilayers as reported previously (28).

The 14:1PC, 16:1PC, 18:1PC, and 20:1PC were purchased from Avanti Polar Lipids (Alabaster, AL); the 18:1PG was purchased from Sigma (St. Louis, MO). Apart from the pure phospholipid bilayer systems, a mixed bilayer system was prepared consisting of 18:1PC and 18:1PG in a 4:1 molar ratio, which will be denoted as 18:1PC/18:1PG. Highly diluted phospholipid samples were prepared with a mutant protein concentration of $\sim$1 μM. The lipid/protein ratio of all samples was $\sim$1500.

Fluorescence measurements

Fluorescence spectra of the BADAN-labeled mutants in lipid bilayer solutions were recorded using excitation light of 390 nm and an emission detection from 400 to 600 nm, with a 2-nm band pass in both excitation and detection light paths on a Fluorolog 3.22 (Jobin Yvon-Spex, Edison, NJ). Red-edge excitation effects were studied by varying the excitation wavelength between 345 and 405 nm. Steady-state fluorescence anisotropy spectra were recorded using slit widths corresponding to a 5-nm band pass. Analysis of the steady-state spectra was performed using IGOR Pro 3.13 (WaveMetrics, Lake Oswego, OR). All experiments were carried out at room temperature ($\sim$20°C).

The unpolarized fluorescence spectra were corrected for the wavelength-dependent sensitivity of the detection system. They also were digitally corrected for background signals by subtracting the spectrum of a sample containing wild-type protein that had approximately the same protein concentration and lipid/protein ratio. The fluorescence anisotropy, $r(\lambda)$, was calculated directly from the uncorrected, polarized fluorescence, $I(\lambda)$, as follows:

$$r(\lambda) = \frac{I(\lambda)_{VV} - G(\lambda)I(\lambda)_{VH}}{I(\lambda)_{VV} + 2G(\lambda)I(\lambda)_{VH}}, \quad G(\lambda) = \frac{I(\lambda)_{HV}}{I(\lambda)_{HH}}, \qquad (1)$$

where the subscript-values refer to the horizontal or vertical settings of the excitation and emission polarizers, respectively. $G(\lambda)$ compensates for the wavelength-dependent, polarizing effects of the instrument.

RESULTS AND DISCUSSION

Fluorescence anisotropy

To acquire the steady-state fluorescence anisotropy, a selection of BADAN-labeled M13 coat protein mutants covering the entire primary amino acid sequence in 18:1PC/18:1PG bilayers was studied by exciting the BADAN label around its absorption maximum (385 nm). This resulted in values for the fluorescence anisotropy r at the fluorescence maximum ranging from $\sim$0.30 for mutant positions in the transmembrane protein region to $\sim$0.25 for positions in the N-terminal region. The anisotropy values were relatively close to the fundamental anisotropy of a related fluorophore LAURDAN, which is $\sim$0.35 in a vitrified solvent (15,21). Similar high anisotropy values were also reported for Aladan-containing globular proteins (13).

The values for the fluorescence anisotropy r found for our protein-lipid system were high compared to what we measured for BADAN in methanol ($r = 0.01$). This indicated that the motion of the BADAN label attached to the labeled protein was restricted. As shown in Fig. 1, the excitation dipole is parallel to the chain that linked the label and protein together (16,29). It is reasonable to assume that the emission dipole has the same orientation. Thus, local dynamics (e.g., rotation around the linker axis) might occur without observing a loss of polarization. The fact that close to both termini (positions 3 and 47) a relatively high anisotropy value also was obtained ($\sim$0.25), suggests that the wobbling motion of the label was restricted throughout the entire protein. For example, a dynamic random coil at both termini would have reduced the anisotropy values considerably. Therefore, the anisotropy data were consistent with our previous finding

that the coat protein comprised an almost straight α-helix (3,11) with an unstructured, nondynamic N-terminal domain from amino acid residues 1–9 (4,5,30) because, in such a conformation, one expects the label to show restricted flexibility.

Fitting of fluorescence spectra

In contrast to the fluorescence spectra of membrane-embedded, AEDANS-labeled M13 coat protein mutants that consist of a single Gaussian line shape (9,10), the fluorescence spectra of BADAN-labeled M13 coat protein mutants are complex line shapes. This is related to differences in the time scale of the excited-state processes compared to the fluorescence life time, which is shorter for BADAN ($\leq$5 ns) than for AEDANS (10–20 ns) (31). As a consequence, the distribution of fluorescent BADAN species is heterogeneous. The fluorescence spectra of membrane-embedded, BADAN-labeled M13 coat protein mutants therefore show variations in position, shape, and width resulting from these phenomena. Because several parameters influence the final energy of the excited states, the wavelength of maximum fluorescence is not a useful parameter for the environmental polarity, as is the case for the AEDANS label (7,9,10).

In all cases, we demonstrated that the fluorescence spectra of BADAN-labeled M13 coat protein mutants could be decomposed into three Gaussian line shapes, each characterized by a position (P), intensity (I), and width (W). In the course of this fitting analysis, we found that the position of two components could be fixed at 23,000 and 22,000 cm^{-1}, respectively, which considerably simplified the spectral decomposition. Typical fitting examples are shown in Fig. 2, for the BADAN label positioned close to the bulk water phase (G3C), in the N-terminal domain located in the phospholipid headgroup region (F11C), and the transmembrane domain embedded within the hydrophobic core region of the bilayer (G38C). High-quality fits were obtained, as was judged from the cor-

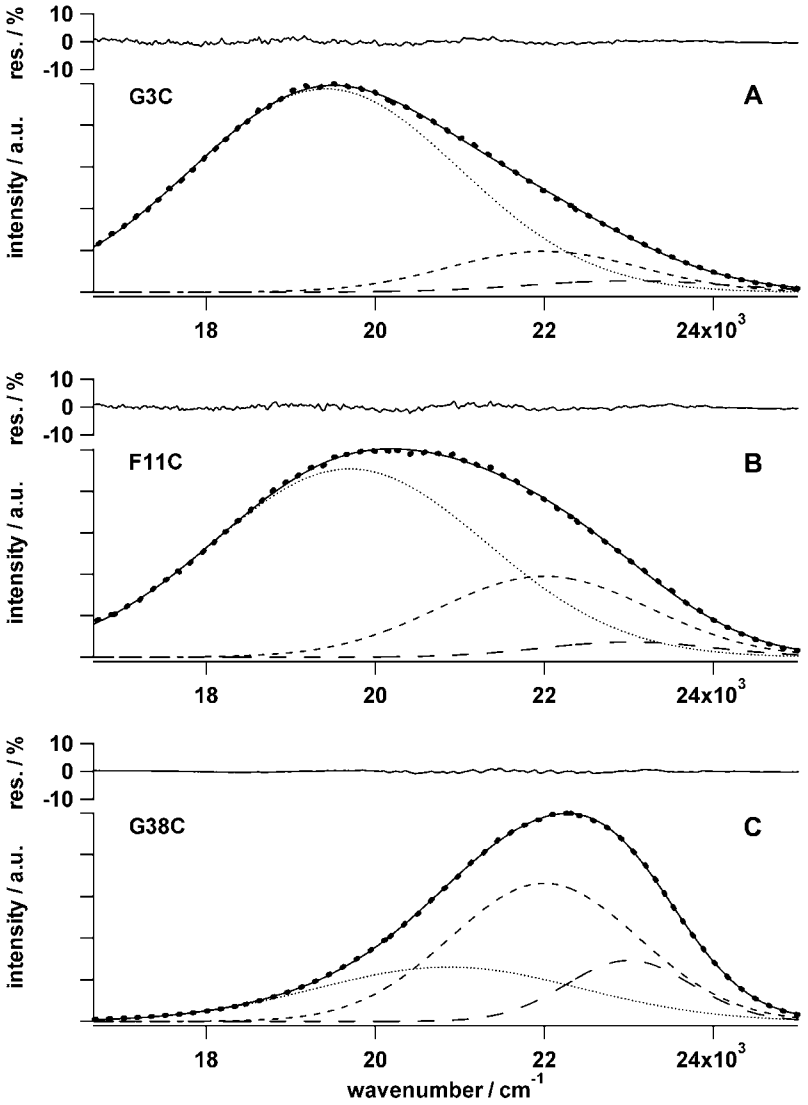

FIGURE 2 Gaussian decomposition of fluorescence spectra of BADAN-labeled mutants G3C (*A*), F11C (*B*), and G38C (*C*) in 18:1PC/18:1PG bilayers (*large dots*) including the fit (*solid line*). The position of the Gaussian line shapes at 23,000 cm^{-1} (*long dashes*) and 22,000 cm^{-1} (*small dashes*) is fixed. The position of the high-wavenumber component (*small dots*) is fitted. Residual plots are scaled between $\pm$10% of the spectral intensity.

responding residual plots in Fig. 2. All other mutants showed fits of similar quality, demonstrating that the spectral decomposition model works well for all cases studied.

A two- or three-component decomposition has been carried out in previous analyses of the fluorescence spectra of a similar fluorophore LAURDAN in biological membranes (32), gel and liquid crystal-phase lipid bilayers (33), and reversed micelles (21). Our spectral decomposition can be related to the proposed energy level scheme of BADAN illustrated in Fig. 3, which schematically shows the heterogeneity of the ground state of BADAN leading to a spectral heterogeneity. The ground state heterogeneity results from differences in hydrogen-bonding capacity of BADAN (Fig. 1) in polar and apolar environments that subsequently will affect the various excited states.

It has been shown in the literature for PRODAN and LAURDAN, which are structurally equivalent to BADAN, that hydrogen bonding results in a lowering of the ICT state to a hydrogen-bonded intramolecular charge transfer (HICT) state (14,15,18,22). By this hydrogen bonding, it is believed that, in the excited state, the negative charge on the carbonyl moiety, which belongs to the electron acceptor part of the BADAN molecule, is stabilized. It should be noted that we excluded the so-called locally excited (Franck-Condon) state in the energy level scheme in Fig. 3, because it can be assumed that the charge transfer process itself is very fast (15,21).

In connection with the fluorescence spectrum of LAURDAN in low-water gel-phase lipid systems with a maximum around 435 nm (~23,000 cm^{-1}) (22,23,33), we assigned the fluorescence component at this position to a nonhydrogen-bonded ICT species (Fig. 3). We could fix its position because it can be assumed that the ICT state is not subjected to solvent relaxation by water molecules in the absence of hydrogen-bonding water (for simplicity, we neglected possible planar intramolecular charge transfer state to twisted intramolecular charge transfer state conversions for the ICT state). In an aqueous environment, the BADAN label would be primarily hydrogen-bonded. Therefore, the contribution of the ICT state in the decomposition was small, as can be seen for BADAN positions close to the bulk water phase (G3C; Fig. 2 *A*) and in the headgroup region (F11C; Fig. 2 *B*).

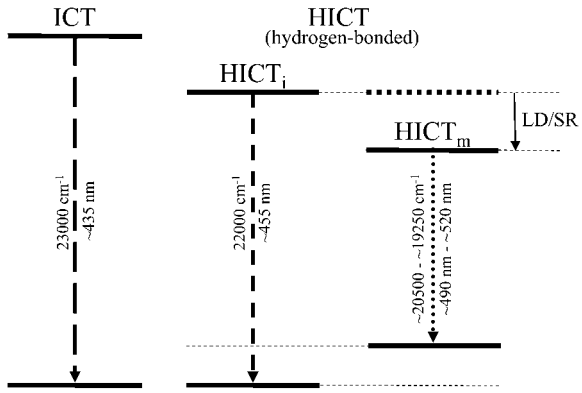

FIGURE 3 Schematic energy level diagram of BADAN showing the nonhydrogen-bonded ICT state and hydrogen-bonded HICT states in an immobilized environment ($HICT_i$) and in a mobile environment ($HICT_m$). The energy difference between the latter two results from solvent relaxation (SR) by water molecules and internal label dynamics (LD). The style of the vectors illustrating the emission corresponds with the style of the fluorescence components in Fig. 2.

For LAURDAN, in highly viscous ethanol at a low temperature (−110°C), a fluorescence spectrum with a maximum of ~450 nm is found (15). We may assume that this fluorescence originates from an HICT state and that solvent relaxation is very slow in this system (15). Based on this observation, it is reasonable to propose that BADAN will show a similar state in lipid systems if it is surrounded by immobilized water molecules. Indeed, from fitting our fluorescence spectra without fixing the position of the fluorescence components (results not shown), the position of one component was consistently found at ~455 nm (22,000 ± 200 cm^{-1}). Therefore, we decided to fix the position of this component for all spectral decompositions at 22,000 cm^{-1}. Because it represents BADAN in an immobilized hydrogen-bonding environment, it is denoted by $HICT_i$ (Fig. 3). A similar fluorescence component is also found in relatively highly ordered gel-phase lipid bilayers for LAURDAN (33) and buried in a globular protein core for Aladan (13).

It is also reported in the literature that increasing the temperature of solutions of LAURDAN in ethanol from −110° to 20°C, the fluorescence spectrum gradually evolves into one with its maximum ~490 nm (15). Clearly, the fluorescence properties of this label change with increasing mobility of its environment. De Vequi-Suplicy et al. found a similar fluorescence component for LAURDAN in liquid crystalline-phase lipid bilayers (33). However, it should be noted that these authors could not discriminate between contributions of internal label dynamics and solvent relaxation based on their data. For BADAN-labeled M13 coat protein in a heterogeneous lipid-water environment with free water molecules in the bulk phase and bound water in the phospholipid headgroup region of the lipids, one might also expect fluorescence contributions from hydrogen-bonded species in both a mobile and (partly) immobilized environment, respectively. Therefore, in a first approximation, we will describe the spectral contribution of hydrogen-bonded BADAN by two fluorescence contributions, one representing the immobile state ($HICT_i$) and one representing the mobile state ($HICT_m$). Apart from internal label dynamics, solvent relaxation (i.e., reorientation of the dipoles of the water molecules) should lower the energy of the initial excited state of hydrogen-bonded BADAN labels, if the rotational correlation time of the water molecules is much shorter than the lifetime of the excited state (~5 ns). This lowering effect is strongly dependent on the physicochemical state of the BADAN environment, so that the final energy of the $HICT_m$ state and related wavelength of emission (i.e., fluorescence Stokes shift) varies with the local polarity as described by the Lippert equation (34).

Interestingly, for BADAN positions within the hydrophobic core region of the phospholipid bilayer, a basically similar three-component decomposition is found as for positions outside the bilayer. The occurrence of the fluorescence components at 23,000 and 22,000 cm^{-1} supports the idea that, in an apolar environment, the ICT and $HICT_i$ states also are present. As may be expected, the contribution of the nonhydrogen-bonded ICT state increased with respect to BADAN positions in an aqueous environment (G38C; Fig. 2 *C*). However, the presence of the hydrogen-bonded $HICT_i$ state was surprising and suggests that, even within the apolar hydrophobic core region of the membrane, the BADAN labels are water bonded, probably in a 1:1 complex as shown in Fig. 1. A large binding constant for a 1:1 complex of LAURDAN and ethanol in cyclohexane was demonstrated previously (14). In this case, the third component with variable wavenumber cannot arise from a lowering of the energy of the $HICT_i$ state by mobile water molecules. Furthermore, the mobile acyl chains of the phospholipids cannot cause a solvent relaxation effect on the charge-transfer excited state, because their dipole moment is too small. Therefore, we assigned the lowering effect of the $HICT_i$ state in the hydrophobic core region to internal label dynamics by twisting of the BADAN molecule in the excited state (i.e., rotation or wobbling of the propanoyl moiety with respect to the aromatic ring; Fig. 1, *arrow*). In this case, the final energy of the $HICT_m$ state would depend on the internal label dynamics of the BADAN molecule attached to the protein.

In the case of water-exposed BADAN labels, it could be expected that internal label dynamics of the molecule might also lower the energy of the $HICT_i$ state. These processes take place simultaneously with solvent relaxation by water molecules and, in our present steady-state approach, we were unable to discriminate between these processes.

In summary, the fluorescence spectra of membrane-embedded BADAN-labeled M13 coat protein mutants were decomposed into three fluorescence components, representing the fluorescence of: 1), nonhydrogen-bonded BADAN; 2), hydrogen-bonded BADAN in an immobile environment; and 3), hydrogen-bonded BADAN either having an internal label dynamics in a mobile aqueous environment for label positions outside the hydrophobic core of the lipid bilayer or with only internal label dynamics for label positions inside the core. Our spectral decomposition enabled us to study the effect of lipid headgroup charge and lipid chain length on three key BADAN fluorescence parameters:

- f_{HB}: Total spectral fraction originating from hydrogen-bonded BADAN labels (sum of contribution of $HICT_i$ and $HICT_m$).
- f_m: Spectral fraction originating from mobile state hydrogen-bonded BADAN labels (contribution of $HICT_m$).
- P_m: Wavenumber position of the mobile state fluorescence component ($HICT_m$), which describes the fluorescence of the final relaxed state and is affected by internal dynamics of the label in the excited state and local polarity effects.

The fractions of the spectral components were calculated by taking the product of the corresponding intensity I and width W relative to the total. From the fit analyses, we found that the standard deviation of the parameters f_{HB} and f_m for BADAN in the N- and C-terminal protein domain is ~0.01. In the transmembrane protein domain, the standard deviation is somewhat greater (i.e., 0.05). However, the standard deviation of P_m strongly depends on the spectral fraction f_m. For values of $f_m \sim 0.9$, the standard deviation in P_m is 10 cm^{-1}. For f_m values of 0.5 and 0.2, this is 100 and 500 cm^{-1}, respectively.

To confirm the spectral decomposition approach, red-edge excitation experiments were carried out for a selection of BADAN-labeled M13 coat protein mutants covering the entire primary amino acid sequence. For most mutants, changing the excitation wavelength from 345 to 405 nm resulted in a small red shift of P_m, and increases of f_{HB} and f_m. Obviously, by optical selection of BADAN labels having an environment more favorable for relaxation of their polar excited state, the probability of exciting hydrogen-bonded species increases. Consequently the spectral contribution of the solvent-relaxed mobile state increases.

Effect of label position

The effect of label position is shown in Fig. 4, *A–C*, where we plotted the BADAN fluorescence parameters (f_{HB},f_m and P_m) for all 40 membrane-embedded BADAN-labeled M13 coat protein mutants in 18:1PC bilayers. From these plots, one can note that the BADAN fluorescence parameters change dramatically around amino acid positions 25 and 40. This finding agrees with previous studies in which it was demonstrated that the transmembrane α-helical domain of the protein runs approximately from residue 21 to 45 (1). Several factors determine the plots in Fig. 4, *A–C*, some of which are related to the structure and the membrane-embedment of the M13 coat protein: tilt, orientation, and depth of insertion. Other factors affect the photophysical state of the BADAN label: local polarity, mobility of environment, internal dynamics of the label, and hydrogen-bonding capacity. Altogether these factors give rise to irregular oscillations of the parameters in Fig. 4, *A–C*. To disentangle the various effects, we assumed the protein to be a perfect α-helix (3–5) and calculated the distance to a reference position at the center of the bilayer, using the known tilt angle, protein orientation, and depth of insertion (10). The center of the BADAN label was taken 7 Å normal to the helical axis, and its position at the virtual amino acid residue number 32.6 (i.e., helical side exactly holding position 29 and exactly opposite to position 38) was taken as the reference position at the center of the bilayer (10). This resulted in the plots in Fig. 4, *D–F*, which express the BADAN fluorescence parameters now as a

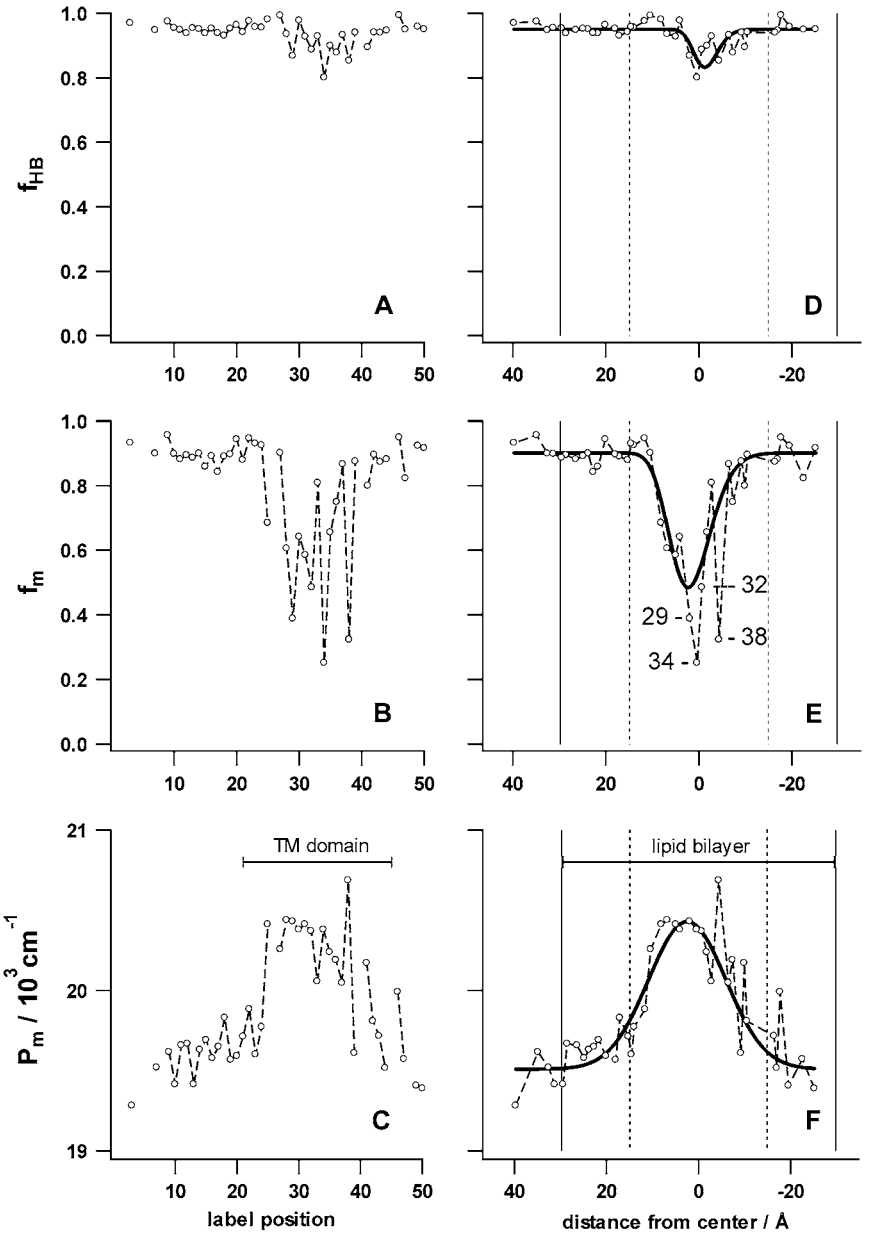

FIGURE 4 BADAN fluorescence parameters f_{HB} (*A* and *D*), f_m (*B* and *E*), and P_m (*C* and *F*) for 40 different mutants in 18:1PC bilayers versus label positions (*A–C*) and versus distance from center (*D–F*). The transmembrane (TM) protein domain runs from label position 21 to 45 (1). The solid vertical lines represent the full bilayer thickness (59.5 Å); the dotted vertical lines represent the acyl chain/glycerol backbone interfaces (the hydrophobic thickness is 29.5 Å) (37,42). The solid trend lines are Gaussian fits to the data points, excluding the strongly scattered data points from positions 29, 34, and 38 (*E*) and positions 38, 41 and 46 (*F*) (see text).

function of the distance to the center of the bilayer. In these plots, the photophysical parameters of the BADAN label primarily played a role.

As can be seen in Fig. 4 *D*, BADAN is fully hydrogen-bonded at all label positions, except for positions in the center of the hydrophobic core of the bilayer, where the spectral fraction of hydrogen-bonded BADAN (f_{HB}) is slightly decreased (by ~20%). This decrease is in agreement with the low water concentration in the bilayer interior as found from molecular dynamics simulations (35,36) and in the structure of a fluid 18:1PC bilayer determined by the joint refinement of x-ray and neutron diffraction data (37). As discussed previously, it can thus be assumed that, in most cases, the BADAN labels are water bonded (Fig. 1).

Also, the spectral fraction originating from mobile state hydrogen-bonded BADAN labels (f_m) is close to 1 for all positions in the water phase and phospholipid headgroup region, but drops to ~0.5 in the hydrophobic core of the bilayer (Fig. 4 *E*, *trend line*). However, label positions 29, 34, and 38 show much lower values. Clearly, for label positions outside the hydrophobic core of the lipid bilayer, the BADAN label is sensing mainly a mobile environment, e.g., both the internal label dynamics and water mobility are relatively high. On moving to the hydrophobic bilayer interior, the local environment of the BADAN label becomes more rigid; internal label dynamics is sufficient to become the relaxation mechanism of the excited HICT state for only ~50% of the BADAN labels. Internal label dynamics as the origin of

the relaxation of the excited state (from ~22,000 to 20,500 cm^{-1}) is confirmed by our observation that increasing the temperature has no effect on P_m at position 29 in the core, but increases f_m from 0.38 to 0.61 (data not shown).

The strongly reduced values for label positions 29, 34, and 38 (position 32 also falls in this group) indicate a reduction of the number of labels with internal label dynamics. It is interesting to note that, for the tilted membrane-embedded protein, positions 29 and 38 exactly face the tilt (e.g., 29 on one side and 38 opposite to that side). In addition, in an α-helical protein model, position 32 is close to 29, and position 34 is close to 38. Consequently, all these BADAN labels are placed ''above'' or ''below'' the protein, directly facing the termini of the acyl chains of the phospholipids. These positions can be expected to sense an increased local lipid ordering and reduced lipid mobility compared to positions at the other sides of the protein helix. This ordering effect will reduce the internal label dynamics and, consequently, lead to a reduced mobile BADAN fraction. This result agrees well with recent findings from a site-directed spin labeling electron spin resonance study of the same protein-lipid systems that the so-called normalized free rotational space of the spin label is reduced around the above-mentioned positions in the center of the transmembrane domain (30). Amino acid positions 29 and 34 especially show strongly reduced values for the normalized free rotational space, which is in excellent agreement with the BADAN data. This finding shows that acyl chains are exerting forces on tilted membrane-bound proteins that can be monitored by measuring the fluorescent properties of BADAN labels.

The wavenumber position of the mobile state fluorescence component (P_m) is shown in Fig. 4 *F*. Because in the data in Fig. 4, *D–F*, we have eliminated the structural effects of the protein-lipid system, the remaining dependence of label depth in the bilayer will result from mainly local polarity effects (i.e., the local dielectric constant ε) as sensed by the BADAN label. Thus, a low or high value of P_m corresponds to a polar or an apolar environment, respectively. The trend line through the data shows a profile over the phospholipid bilayer that roughly follows the water penetration in the phospholipid bilayer (37,38), resulting in a concomitant change in local dielectric constant ε. On top of this profile, deviations are again observed in the hydrophobic core of the lipid bilayer, especially for label positions in the C-terminal part of the transmembrane protein domain. These label positions are close to the three lysine residues (Lys40, Lys43, and Lys44) and two phenylalanine residues (Phe42 and Phe45) that provide a very strong anchoring domain for the C-terminal part of the protein (1). The presence of this anchoring domain could result in a change of local water distribution or lipid packing.

For simplicity, we have assumed that the M13 coat protein can be described by a full α-helix. However, previous work has demonstrated that the amino acid residues 1–9 are unstructured (4,5,30). These amino acid positions are located on the N-terminal hydrophilic anchor that is emerging from the headgroup region into the water phase, given by distances from the bilayer center >30 Å in Fig. 4 *F* (4). The presence of an unstructured protein domain explains the limited fit to the data in this water-lipid region. The fluorescence maximum for PRODAN in water is ~530 nm (18,860 cm^{-1}). For position 3, we found a higher value for P_m of 19,200 cm^{-1}. This indicates that, even at the N-terminal end of the membrane-embedded protein, the BADAN labels are not sensing a bulk water environment, probably due to the fact that the BADAN label has a short linker to the protein backbone.

In conclusion, the analysis of the BADAN fluorescence parameters (f_{HB}, f_m, and P_m) demonstrated that most of the fluorescence originates from BADAN labels that are hydrogen bonded to water molecules even within the hydrophobic core of the membrane. The data are consistent with a tilted membrane-embedded structure of the M13 coat protein and a Gaussian profile for the dielectric constant ε over the membrane.

Effect of headgroup charge

The effect of headgroup charge was studied by comparing all 40 BADAN-labeled protein mutants in pure 18:1PC and mixed 18:1PC/18:1PG bilayers (Fig. 5). The effect of headgroup charge is a small increase of the spectral fraction of hydrogen-bonded BADAN (f_{HB}) (Fig. 5 *A*). In the transmembrane protein domain (i.e., label positions in the core of the membrane), the effect of headgroup charge on the spectral fraction of mobile state hydrogen-bonded BADAN labels (f_m) is small (Fig. 5 *B*). However, for label positions in the C- and N-terminal domain (label positions 10–24 and 42–50), which are in the headgroup region, a consistent decrease on f_m is seen on addition of the negatively charged 18:1PG to pure 18:1PC. This indicates a decrease of mobility of the local environment, which most likely results from an increase in bound water molecules at the negatively charged headgroup region. Water molecules in the headgroup region are motionally restricted by hydrogen bonding with lipid headgroups, which is confirmed by the observation that P_m of mutant A18C decreases upon increasing temperature from 20° to 70°C (data not shown). This decrease of P_m indicates an increase of relaxation by water becoming more dynamic at higher temperatures. In contrast, the value of P_m of mutant G3C did not change with increasing temperature, as might be expected, because the N-terminus has been shown previously to reside in the highly mobile water phase (4). Recent results of molecular dynamics simulations (39) also demonstrate that hydrogen bonding to the glycerol group of 1-palmitoyl-2-oleoyl-phosphatidylglycerol slows down water motion more than the choline group of POPC (1-palmitoyl-2-oleoyl-phosphatidylcholine).

Overall the BADAN fluorescence spectrum is slightly red shifted for mixed 18:1PC/18:1PG compared to pure 18:1PC. This is reflected by a decrease of P_m as seen in Fig. 5 *C* for

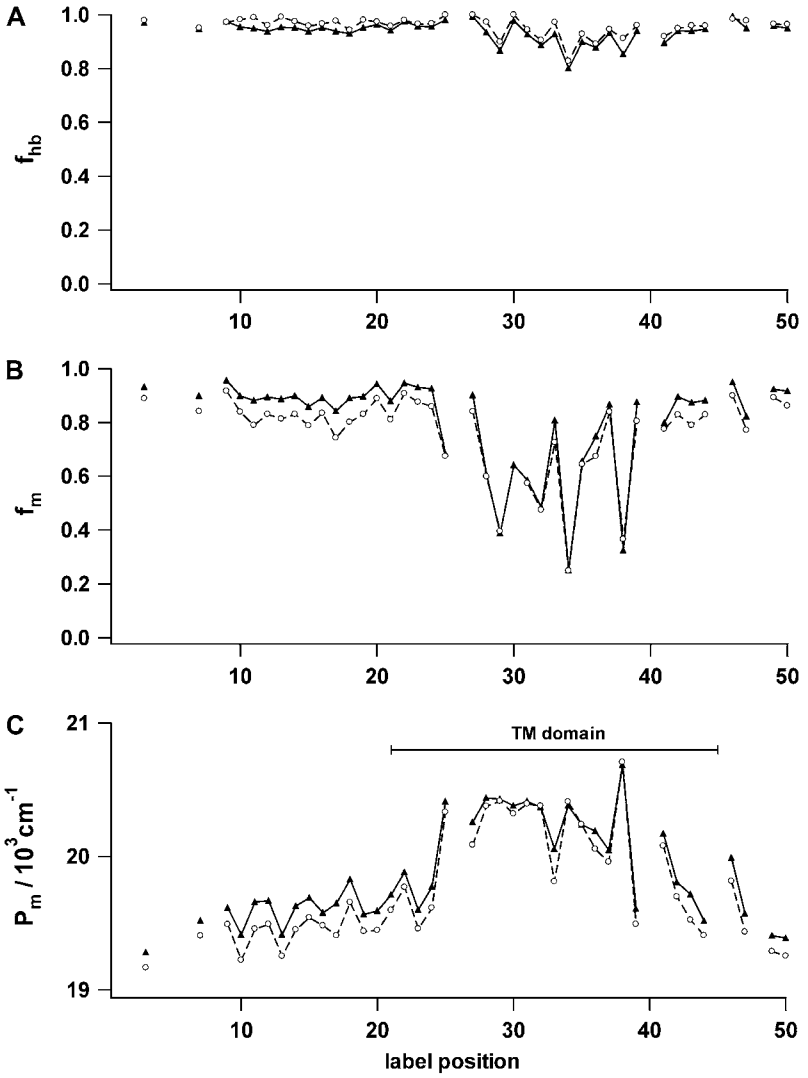

FIGURE 5 BADAN fluorescence parameters f_{HB} (*A*), f_m (*B*), and P_m (*C*) for 40 different mutants (position of labeled cysteine on *horizontal axis*) as function of the composition of the lipid headgroup region (18:1PC, ▲; 18:1PC/18:1PG, ○). The transmembrane (TM) domain runs from position 21 to 45 (1). Data points for adjacent label positions are connected by a line.

almost all label positions. This decrease indicates an overall increased polarity, which is in agreement with an enhanced hydration level of the membrane resulting from an increased intermolecular spacing of the phospholipid headgroups (23). This enhanced hydration level is also in agreement with the increase of f_{HB} in Fig. 5 *A*.

However, in Fig. 5, no shift in the patterns of the BADAN fluorescence parameters is seen compared to the length and position of the putative transmembrane domain, indicating that changing the charge of the phospholipid headgroups under the current conditions does not affect the topology and membrane-embedment of the M13 coat protein.

Effect of lipid chain length

The effect of increase of phospholipid acyl chain length on going from 14:1PC to 20:1PC on the BADAN fluorescence parameters (f_{HB}, f_m, and P_m) is shown in Fig. 6 for all 40 membrane-embedded BADAN-labeled protein mutants. It should be noted that, under the experimental conditions (room temperature), all bilayer systems are in the liquid crystalline phase, as the gel-to-liquid crystalline phase transition temperature of the thickest 20:1PC is ~−5°C (40). It can be seen that, for mutant positions in the N-terminal domain or at the C-terminal domain (i.e., in the headgroup regions and bulk water), f_{HB} and f_m are close to 1, irrespective of bilayer thickness (Fig. 6, *A* and *B*). This indicates that the hydrogen-bonding capacity of the BADAN label and its internal dynamics in this region of the lipid-water system are not affected by a change in bilayer thickness. This is in agreement with molecular dynamics results showing that the water diffusion coefficient is not affected by bilayer thickness (41).

In contrast, f_{HB} and f_m decrease upon increasing acyl chain length for label positions in the transmembrane region, the effect of which is substantially greater for f_m. The relatively small decrease of f_{HB} for positions in the center of the transmembrane region in the bilayer center on increasing acyl chain length (Fig. 6 *A*) indicates a reduction of the fraction of hydrogen-bonded BADAN labels in the bilayer. The decrease suggests more apolar character and a reduced water

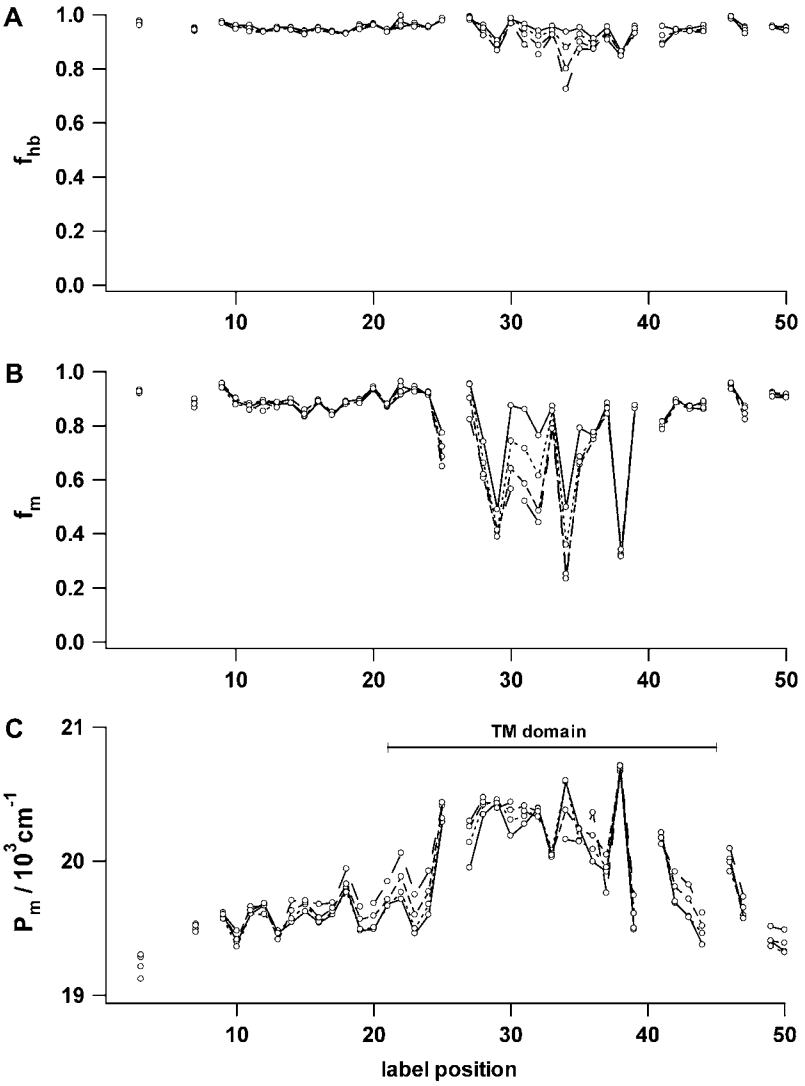

FIGURE 6 BADAN fluorescence parameters f_{HB} (*A*), f_m (*B*), and P_m (*C*) for 40 different mutants (position of labeled cysteine on *horizontal axis*) as function of lipid acyl chain length (14:1PC, *solid line*; 16:1PC, *dotted line*; 18:1PC, *small dashes*; 20:1PC, *long dashes*). The transmembrane (TM) protein domain for 18:1PC is indicated (Fig. 5). Data points for adjacent label positions are connected by a line.

concentration in the hydrophobic core of thick bilayers compared to thin bilayers. This is in agreement with the finding of a reduced water permeability on increasing acyl chain length that has been demonstrated by molecular dynamics simulations (41).

The spectral fraction originating from mobile state hydrogen-bonded BADAN labels (f_m) in the transmembrane region is affected mainly by the internal label dynamics of the BADAN labels. As discussed above, BADAN label positions that are ''above'' or ''below'' the α-helical transmembrane protein domain are directly facing the termini of the acyl chains of the phospholipids. They therefore sense a higher local lipid ordering and reduced lipid mobility compared to positions at the other sides of the protein helix. This effect becomes stronger when the acyl chains are longer, even though the tilt will reduce in this case (10).

The effect of phospholipid acyl chain length on the wavenumber position of the mobile state fluorescence component (P_m) is shown in Fig. 6 *C*. As discussed previously, P_m depends primarily on the local polarity (i.e., the local dielectric constant ε) that is sensed by the BADAN label. For all lipid systems, there is a sharp increase in P_m in the N-terminal domain around label position 25. At the C-terminal domain, a similar effect is seen between positions 41–50. These changes of P_m reflect the drop in local polarity at positions where the transmembrane protein enters and leaves the apolar hydrophobic core region of the bilayer. It is interesting to note that these positions remain the same, irrespective of the bilayer thickness. This observation indicates that the protein responds to a change in bilayer thickness by a change in tilt angle, thereby keeping the transmembrane domain embedded in the bilayer as much as possible. This conclusion is in agreement with previous work (10).

Upon increasing the phospholipid acyl chain length on going from 14:1PC to 20:1PC, a consistent increase of P_m is observed for BADAN label positions in the N-terminal domain from 13 to 25 (Fig. 6 *C*). These positions are mainly located in the headgroup region of the phospholipid bilayers.

The increase of P_m indicates that, on increasing the hydrophobic thickness, the BADAN label will gradually experience a less polar environment. The same phenomenon may be seen when comparing the data for label positions 41–50 in the C-terminal domain at the opposite headgroup region of the bilayer. As discussed for the headgroup charge effects, this indicates a reduced hydration level on increasing the acyl chain length close to the glycerol/acyl chain interface.

In conclusion, we have presented a new and simple method based on site-directed fluorescence labeling using the BADAN label that enables the examination of protein-lipid interactions in great detail. By using our three-component spectral model, we can separate Stokes shift contributions from water and internal label dynamics, and protein topology. The method can reveal the embedment of the labeled protein in the membrane bilayer, as well as key characteristics of the membrane, such a hydration level and local polarity (i.e., the local dielectric constant ε).

REFERENCES

1. Stopar, D., R. B. Spruijt, and M. A. Hemminga. 2006. Anchoring mechanisms of membrane-associated M13 major coat protein. *Chem. Phys. Lipids.* 141:83–93.
2. Fernandes, F., L. M. S. Loura, M. Prieto, R. Koehorst, R. B. Spruijt, and M. A. Hemminga. 2003. Dependence of M13 major coat protein oligomerization and lateral segregation on bilayer composition. *Biophys. J.* 85:2430–2441.
3. Vos, W. L., R. B. M. Koehorst, R. B. Spruijt, and M. A. Hemminga. 2005. Membrane-bound conformation of M13 major coat protein: a structure validation through FRET-derived constraints. *J. Biol. Chem.* 280:38522–38527.
4. Nazarov, P. V., R. B. M. Koehorst, W. L. Vos, V. V. Apanasovich, and M. A. Hemminga. 2007. FRET study of membrane proteins: determination of the tilt and orientation of the N-terminal domain of M13 major coat protein. *Biophys. J.* 92:1296–1305.
5. Vos, W. L., M. Schor, P. V. Nazarov, R. B. M. Koehorst, R. B. Spruijt, and M. A. Hemminga. 2007. Structure of membrane-embedded M13 major coat protein is insensitive to hydrophobic stress. *Biophys. J.* 93:3541–3547.
6. Marvin, D. A. 1998. Filamentous phage structure, infection and assembly. *Curr. Opin. Struct. Biol.* 8:150–158.
7. Spruijt, R. B., C. J. A. M. Wolfs, J. W. G. Verver, and M. A. Hemminga. 1996. Accessibility and environment probing using cysteine residues introduced along the putative transmembrane domain of the major coat protein of bacteriophage M13. *Biochemistry.* 35:10383–10391.
8. Spruijt, R. B., A. B. Meijer, C. J. A. M. Wolfs, and M. A. Hemminga. 2000. Localization and rearrangement modulation of the N-terminal arm of the membrane-bound major coat protein of bacteriophage M13. *Biochim. Biophys. Acta.* 1508:311–323.
9. Spruijt, R. B., C. J. A. M. Wolfs, and M. A. Hemminga. 2004. Membrane assembly of M13 major coat protein: evidence for a structural adaptation in the hinge region and a tilted transmembrane domain. *Biochemistry.* 43:13972–13980.
10. Koehorst, R. B. M., R. B. Spruijt, F. J. Vergeldt, and M. A. Hemminga. 2004. Lipid bilayer topology of the transmembrane α-helix of M13 major coat protein and bilayer polarity profile by site-directed fluorescence spectroscopy. *Biophys. J.* 87:1445–1455.
11. Nazarov, P. V., R. B. M. Koehorst, W. L. Vos, V. V. Apanasovich, and M. A. Hemminga. 2006. FRET study of membrane proteins: simulation-based fitting for analysis of membrane protein embedment and association. *Biophys. J.* 91:454–466.
12. Cohen, B. E., T. B. McAnaney, E. S. Park, Y. N. Jan, S. G. Boxer, and L. Y. Jan. 2002. Probing protein electrostatics with a synthetic fluorescent amino acid. *Science.* 296:1700–1703.
13. Abbyad, P., X. Shi, W. Childs, T. B. McAnaney, B. E. Cohen, and S. G. Boxer. 2007. Measurement of solvation responses at multiple sites in a globular protein. *J. Phys. Chem. B.* 111:8269–8276.
14. Józefowicz, M., K. A. Kozyra, J. R. Heldt, and J. Heldt. 2005. Effect of hydrogen bonding on the intramolecular charge transfer fluorescence of 6-dodecanoyl-2-dimethylaminonaphtalene. *Chem. Phys.* 320: 45–53.
15. Viard, M., J. Gallay, M. Vincent, O. Meyer, B. Robert, and M. Paternostre. 1997. Laurdan solvatochromism: solvent dielectric relaxation and intramolecular excited-state reaction. *Biophys. J.* 73:2221–2234.
16. Parasassi, T., E. K. Krasnowska, L. Bagatolli, and E. Gratton. 1998. Laurdan and Prodan as polarity-sensitive fluorescent membrane probes. *J. Fluoresc.* 8:365–373.
17. Lobo, B. C., and C. J. Abelt. 2003. Does PRODAN possess a planar or twisted charge-transfer excited state? Photophysical properties of two PRODAN derivatives. *J. Phys. Chem. A.* 107:10938–10943.
18. Samanta, A., and R. W. Fessenden. 2000. Excited state dipole moment of PRODAN as determined from transient dielectric loss measurements. *J. Phys. Chem. A.* 104:8972–8975.
19. Jurkiewicz, P., J. Sýkora, A. Olzyńska, J. Humpolícková, and M. Hof. 2005. Solvent relaxation in phospholipid bilayers: principles and recent applications. *J. Fluoresc.* 15:883–894.
20. Parusel, A. B. J., W. Nowak, S. Grimme, and G. Kohler. 1998. Comparative theoretical study on charge-transfer fluorescence probes: 6-propanoyl-2-(N,N-dimethylamino)naphthalene and derivatives. *J. Phys. Chem. A.* 102:7149–7156.
21. Vincent, M., B. de Foresta, and J. Gallay. 2005. Nanosecond dynamics of a mimicked membrane-water interface observed by time-resolved stokes shift of LAURDAN. *Biophys. J.* 88:4337–4350.
22. Parasassi, T., and E. Gratton. 1995. Membrane lipid domains and dynamics as detected by Laurdan fluorescence. *J. Fluoresc.* 5:59–69.
23. Bagatolli, L. A., E. Gratton, and G. D. Fidelio. 1998. Water dynamics in glycosphingolipid aggregates studied by LAURDAN fluorescence. *Biophys. J.* 75:331–341.
24. Sýkora, J., P. Kapusta, V. Fidler, and M. Hof. 2002. On what time scale does solvent relaxation in phospholipid bilayers happen? *Langmuir.* 18:571–574.
25. Krasnowska, E. K., E. Gratton, and T. Parasassi. 1998. Prodan as a membrane surface fluorescence probe: Partitioning between water and phospholipid phases. *Biophys. J.* 74:1984–1993.
26. Söderlund, T., J.-M. I. Alakoskela, A. L. Pakkanen, and P. K. J. Kinnunen. 2003. Comparison of the effects of surface tension and osmotic pressure on the interfacial hydration of a fluid phospholipid bilayer. *Biophys. J.* 85:2333–2341.
27. Zhang, Y.-L., J. A. Frangos, and M. Chachisvilis. 2006. Laurdan fluorescence senses mechanical strain in the lipid bilayer membrane. *Biochem. Biophys. Res. Commun.* 347:838–841.
28. Spruijt, R. B., C. J. A. M. Wolfs, and M. A. Hemminga. 1989. Aggregation-related conformational change of the membrane-associated coat protein of bacteriophage M13. *Biochemistry.* 28:9158–9165.
29. Celli, A., S. Beretta, and E. Gratton. 2007. Phase fluctuation on the micron-submicron scale in GUVs composed of a binary lipid mixture. *Biophys. J.* 94:104–116.
30. Stopar, D., J. Strancar, R. B. Spruijt, and M. A. Hemminga. 2006. Motional restrictions of membrane proteins: a site-directed spin labeling study. *Biophys. J.* 91:3341–3348.
31. Hammarström, P., R. Owenius, L.-G. Mårtensson, U. Carlsson, and M. Lindgren. 2001. High-resolution probing of local conformational changes in proteins by the use of multiple labeling: unfolding and

self-assembly of Human Carbonic Anhydrase II monitored by spin, fluorescent, and chemical reactivity probes. *Biophys. J.* 80:2867–2885.

32. Vanounou, S., D. Pines, E. Pines, A. H. Parola, and I. Fishov. 2002. Coexistence of domains with distinct order and polarity in fluid bacterial membranes. *Photochem. Photobiol.* 76:1–11.
33. De Vequi-Suplicy, C., C. Benatti, and M. Lamy. 2006. Laurdan in fluid bilayers: position and structural sensitivity. *J. Fluoresc.* 16:431–439.
34. Lakowicz, J. R. 2006. Principles of Fluorescence Spectroscopy, 3rd ed. Springer, New York.
35. Chiu, S. W., E. Jakobsson, S. Subramaniam, and H. L. Scott. 1999. Combined Monte Carlo and molecular dynamics simulation of fully hydrated dioleyl and palmitoyl-oleyl phosphatidylcholine lipid bilayers. *Biophys. J.* 77:2462–2469.
36. Berkowitz, M. L., D. L. Bostick, and S. Pandit. 2006. Aqueous solutions next to phospholipid membrane surfaces: insights from simulations. *Chem. Rev.* 106:1527–1539.
37. White, S. H., and W. C. Wimley. 1998. Hydrophobic interactions of peptides with membrane interfaces. *Biochim. Biophys. Acta.* 1376:339–352.
38. Marsh, D. 2002. Membrane water-penetration profiles from spin labels. *Eur. Biophys. J.* 31:559–562.
39. Murzyn, K., W. Zhao, M. Karttunen, M. Kurdziel, and T. Rog. 2006. Dynamics of water at membrane surfaces: effect of headgroup structure. *Biointerphases.* 1:98–105.
40. Koynova, R., and M. Caffrey. 1998. Phases and phase transitions of the phosphatidylcholines. *Biochim. Biophys. Acta.* 1376:91–145.
41. Sugii, T., S. Takagi, and Y. Matsumoto. 2005. A molecular-dynamics study of lipid bilayers: effects of the hydrocarbon chain length on permeability. *J. Chem. Phys.* 123:184714.
42. Ridder, A. N. J. A., W. van de Hoef, J. Stam, A. Kuhn, B. de Kruijff, and J. A. Killian. 2002. Importance of hydrophobic matching for spontaneous insertion of a single-spanning membrane protein. *Biochemistry.* 41:4946–4952.